Recent Scientific Results from the Chandra HRC GTO Program

Stephen S. Murray[a] and the HRC Science Team
[a]Harvard-Smithsonian Center for Astrophysics
60 Garden Street, MS-2
Cambridge, MA 02138

ABSTRACT

The Chandra X-ray Observatory (CXO) has now been in orbit a little over three years. During that time, the High Resolution Camera (HRC) Science Team has been carrying out a program of science observations making use of all of the capabilities of the Observatory with particular emphasis on the capabilities of the HRC for high resolution timing, and high resolution imaging. In this review of Chandra science, we present highlights of the past three years of observations including detailed studies of the Andromeda Galaxy (M31), discovery of a pulsar in the Supernova Remnant 3C58, and studies of X-ray emission from the nearby AGN Centaurus A.

Keywords: X-ray astronomy, Chandra X-ray Observatory, HRC, pulsars, AGN, galaxies

1. INTRODUCTION

The Chandra X-ray Observatory was launched into orbit on July 23, 1999 aboard the Space Shuttle Columbia (SST-93) and reached it operating orbit (10,000 x 140,000 km) about two weeks later. After systems activation and checkout the first X-rays were observed on August 12, 1999 heralding a new era of high resolution X-ray imaging and spectroscopy. Now slightly more than three years later, Chandra has observed several thousand targets and returned truly unique and outstanding data for scientists around the world to analyze. An overview of the observatory, its complement of science instruments, and performance can be found in an article by Weisskopf et al..[1]

The Chandra observing program includes a guaranteed observing time (GTO) component for the Instrument Principal Investigator (IPI) teams that allows for broad science programs to be carried out during the first several years of the mission. The HRC Science Team* has used the GTO program to obtain both HRC and ACIS (Advanced CCD Imaging Spectrometer) data in various instruments operating modes that test our understanding of the instrument, and extend their overall scientific usefulness. These observations include exciting science such as: detailed studies of the nuclear region of M31, our nearest neighbor spiral galaxy; a search for, and discovery of, a pulsar near the center of the Supernova Remnant 3C58; and resolving the complex X-ray emission from the nearest Active Galactic Nucleus (AGN), Centaurus A.

2. M31 - ANDROMEDA GALAXY: THE NUCLEUS AND A TWO YEAR SYNOPTIC STUDY

The HRC and ACIS detectors on Chandra were used to monitor X-ray emission from the central region of M31, searching for X-ray transients and resolving the complex emission from the nucleus. Figure 1 shows the central region of M31 obtained by summing up 8 individual short exposures (4 to 9 ksec) of the nucleus spread over two years (1999-2001) which were carried out as part of the HRC GTO program. The "true color" shows regions of softest (or cool) emission as red, and hardest (or hot) as blue.

Further author information: (Send correspondence to S.S.M)
S.S.M.: E-mail: ssm@head-cfa.harvard.edu
*The HRC Science Team includes L. David, R. Di Stefano, M. Elvis, G. Fabbiano, W. Forman, M. Garcia, J. Grindlay, F. Harnden, C. Jones, A. Kenter, A. Kong, R. Kraft, M. Markevitch, J. McClintock, F. Seward, P. Slane, H. Tananbaum, A. Vikhlinin, M. Ward
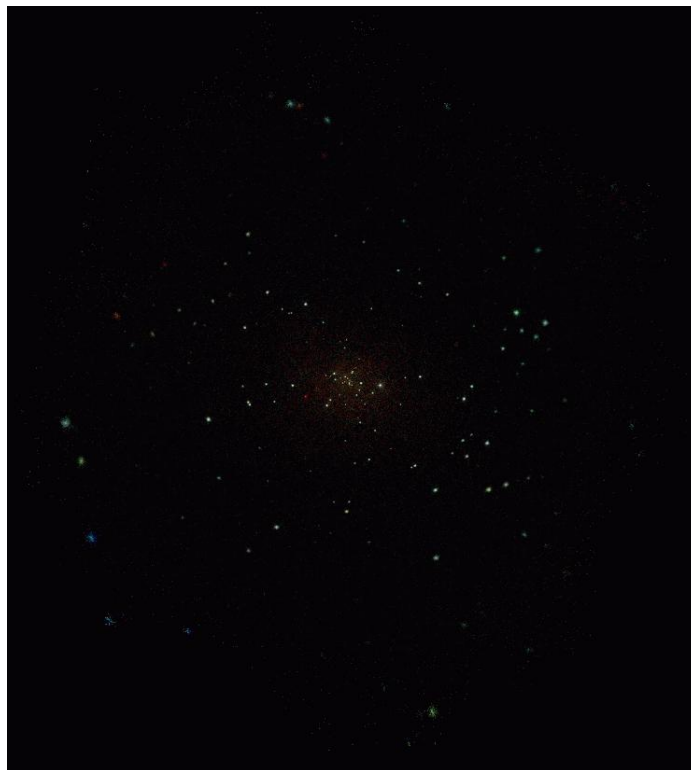
Figure 1. Central Region of M31. This 17x17 arc minute image is made up of 8 individual ACIS-I images taken over two years from 1999-2001. The image is "true color" constructed from the soft (red: 0.3-1 keV), medium (green: 1-2 keV), and hard (blue: 2-7 keV) energy bands. The pixels are 1.93 arc seconds, and the image has been smoothed with a Gaussian (0.5 arc second sigma) function.

2.1. Source Population

Using a wavelet based detection algorithm (WAVEDETECT Freeman et al.[2]) a total of 204 sources are found in this region (Kong et al.[3, 4]). Of these 78 have counterparts in the $ROSAT$ HRI catalog (Primini et al.[5]) while the remaining 126 sources were either below the detection limit of that catalog or are variable. The Chandra stacked image extends ~5 times fainter than the $ROSAT$ catalog, with a limiting sensitivity corresponding to $L_x \sim 2 \times 10^{35}$erg s^{-1} in the inner region of the field where the PSF is smallest. We identify 22 Chandra sources with globular clusters (8 are new), 2 sources are coincident with Supernova Remnants (one is clearly extended), and 8 sources are associated with planetary nebulae (PN). The X-ray luminosities for these PN are much higher than expected. In our galaxy PN detected as X-ray sources have $L_x \sim 10^{30-32}$erg s^{-1}, whereas in M31 $L_x \succeq 10^{35}$erg s^{-1}, suggesting the interesting possibility that these Planetary Nebulae in M31 may be incorrectly classified. For example, these may actually be symbiotic stars with neutron star companions (similar to the galactic source GX 1+4). Future optical spectroscopy may help resolve this puzzle.

There is unresolved emission in the central region of M31 that is easily seen near the center of the image. The spectrum of this emission is relatively low in energy indicating a cool (kT~0.35 keV) temperature. In addition, an extrapolation of the luminosity function of the detected point source population to lower luminosity can not make up the integrated emission of this unresolved component. Thus we conclude that the unresolved emission is diffuse and associated with the Interstellar Medium (ISM) of M31. It appears that this gas cools moving outward from the nucleus of M31 (Dosaj et al.[6]).

2.2. Nuclear Region
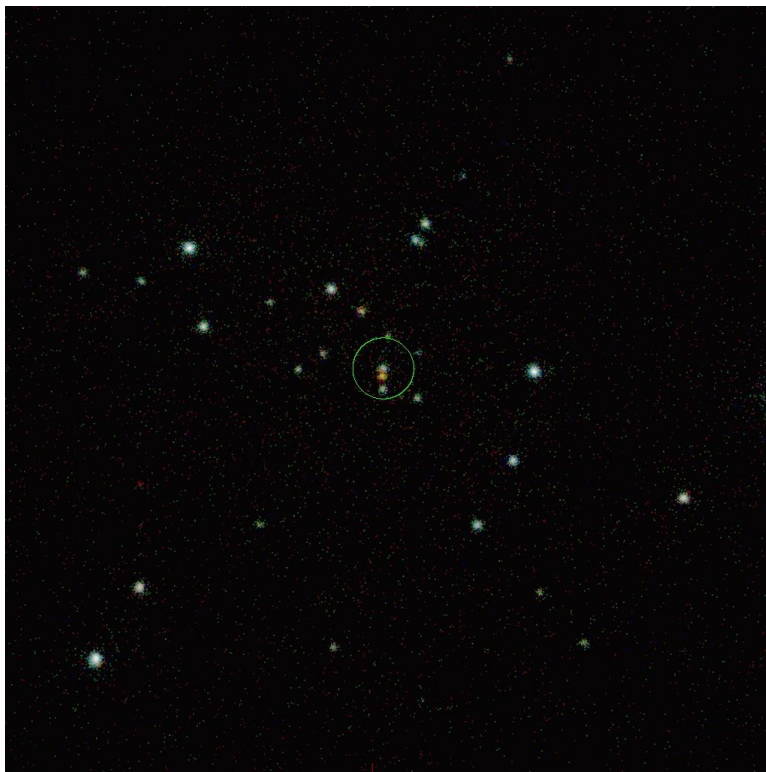
Figure 2. A "true color" image of the central 2x2 arc minutes of M31. The circle is 5 arc seconds in radius and denotes the region near the actual nucleus of M31, which contains 5 previously unresolved X-ray sources.

In Figure 2 we show a more detailed image, again in "true color", of the central 2 arc minutes of M31. The circle shows the central 5 arc second radius region in which at least five x-ray sources are detected. Prior to this Chandra image these sources were unresolved (e.g. *ROSAT* and *Einstein*) and, therefore, an identification of X-ray emission coming from the super massive black hole at the nucleus of M31 was not possible. One of the Chandra sources near to the nucleus has a peculiar X-ray spectrum (Garcia et al.[7]) and in the "true color" image appears red. It is a super soft X-ray source that has the unusual X-ray property of emitting all its flux at low energy (< 1 keV). This type of source is usually associated with a white dwarf, but it is possible that this source, being so near to the central black hole of M31, is somehow associated with the nucleus. We originally suggested this identification, although with some reservations as discussed by Garcia et al..[7] With the use of the Hubble Space Telescope Wide Field/Planetary Camera (HST WF/PC) and the identification of two globular cluster sources in both the HST and Chandra images, we have improved the astrometric precision of the X-ray source locations relative to the nucleus of M31 to about 0.1 arc seconds (Garcia et al.[8]).

As shown in Figure 3 the source north of the super soft source (designated CXO M31 J004244.3+411608) is coincident with M31* within 0.15 arc seconds. The peak X-ray luminosity of M31* during the two years we have observed is $L_x \sim 3 \times 10^{37}$ ergs/sec (the typical luminosity is ~5 times lower), which implies that this central region is not very active and that the $\sim 3 \times 10^7 \mathrm{M}_\odot$ black hole is probably accreting matter at a very low rate (Garcia et al.[8]).

2.3. Variability and Transients

In addition to resolving the complex of X-ray sources near the center of M31, Chandra observations have identified a number of variable X-ray sources, some of which may be associated with transient emission characteristic
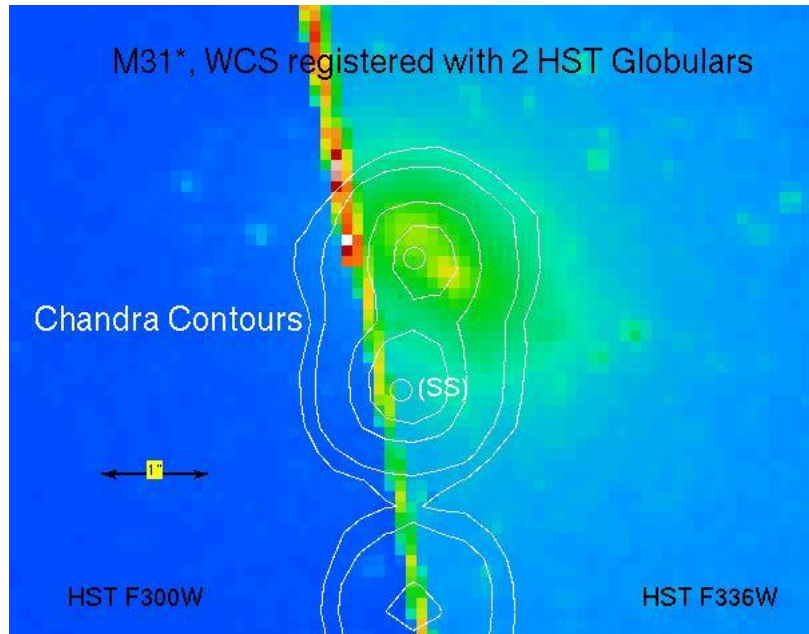
Figure 3. A composite HST image of the nucleus of M31. The two bright regions are P1 and P2, the super massive black hole in the nucleus (M31*) lies between them. Contours from the Chandra stacked image are shown, properly registered, using two HST globular clusters which are also detected with Chandra.

of a population of binary systems containing stellar mass black holes.

Of the 204 sources detected in our observations, 99 are classified as variable (Kong et al.[4]) based on the criteria of Primini et al.,[5] i.e. $S = (L_{max} - L_{min})/\sqrt{\sigma^2_{F_{max}} + \sigma^2_{F_{min}}} \geq 3$. The is weak evidence that the fraction of variable sources decreases moving out from the central region of M31. However, there are various systematic effects and biases (such as faint source detection limits changing with PSF) that need to be evaluated in order to confirm this trend.

About 12 of the variable sources are classified as bright transients according the the criteria that the variability factor $S > 3\sigma$, and there be at least one observation with a luminosity $L_x \succeq 5 \times 10^{36}$erg s^{-1}and one observation where the source is not detected. These criteria were chosen based on the properties of soft X-ray transients (SXT) and Be/X-ray binaries seen in the Milky Way Galaxy. We have observed some of these transient sources with the HST when they are X-ray bright, and again when they become X-ray dim to look for corresponding changes in the optical band to help identify these objects and confirm their classification as black hole candidates. Thus far we have had only modest success, possibly identifying one transient seen in XMM observations which is a super soft source, and one Nova from the Chandra data which became X-ray bright about 6 years after the optical outburst. For two other transients with HST observations we find no optical counterpart to the HST limiting magnitude U=24. The brightest X-ray transient in our survey ($L_x \sim 3 \times 10^{38}$erg s^{-1}) has been seen with HST and we have been able to follow its decay both in the X-ray and optical. Based on the X-ray and optical data, we suspect this is fairly long period low mass binary system containing a stellar mass black hole. On average we are finding one new X-ray transient every time we observe the central region of M31. However, these are typically very faint in the optical (HST U-band) and so in the future we will only follow the brightest X-ray transients ($L_x > 10^{38}$erg s^{-1}), and we will use the ACS on HST to gain about 2 magnitudes in sensitivity for the same exposure time. We anticipate seeing about one of these bright transients per year.
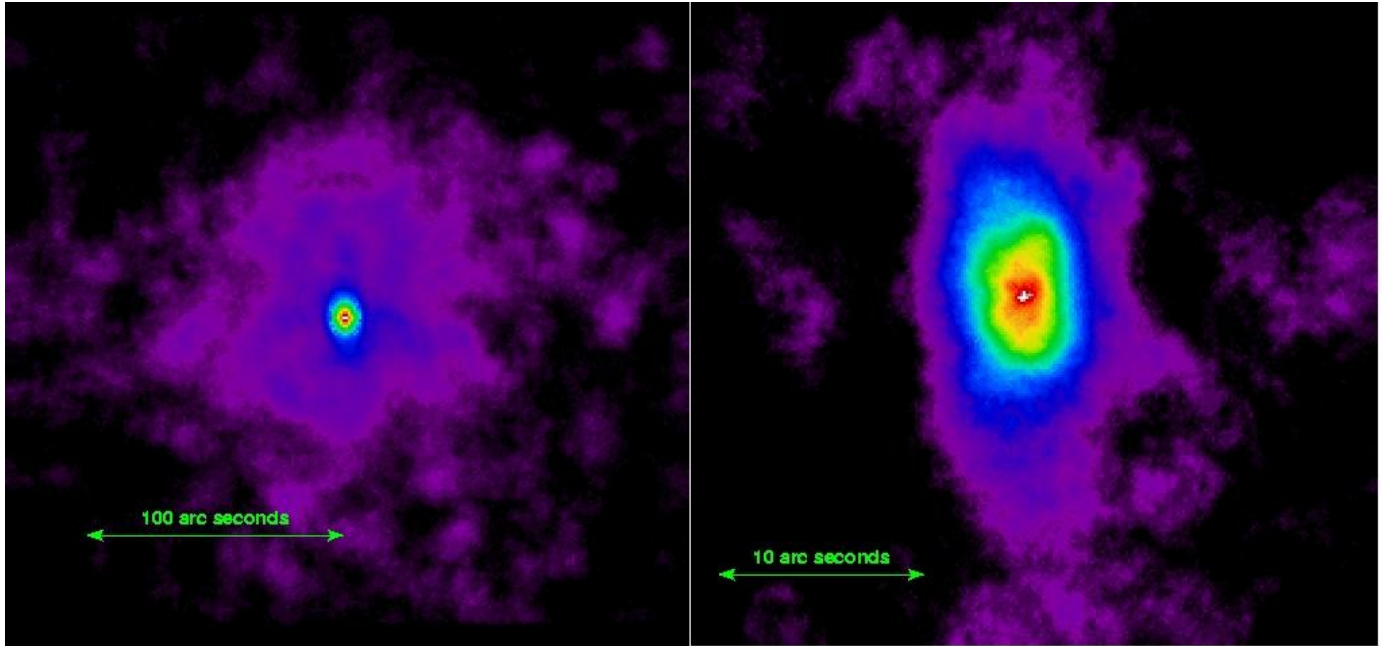
Figure 4. Two views of the Supernova Remnant 3C58. On the left is the SNR nebula with a compact object at the center. The image is an adaptively smoothed image with 1 arc second bins with a smoothing threshold of 200 counts/region. The image on the right is binned at 0.13 arc seconds and adaptively smoothed with a threshold of 40 counts/region.

3. 3C58 - PULSAR SEARCH

The HRC on Chandra is a photon counting detector with the ability to time tag each detected photon with about 16 μsec accuracy. Therefore, this detector is very well suited for detecting period variations in the intensity of an X-ray source. With the very high spatial resolution of the HRC it is possible to select photons from a point source embedded in extended emission, further increasing the sensitivity for detecting period behavior. In the process of using the HRC for timing studies it was found that the jth event time was being assigned to the $(j+1)^{th}$ event, which was traced to a wiring error in the HRC event processing electronics. A work around for this problem, when using the HRC to study short period time phenomena, is to operate the HRC-S with only the central segment active (the HRC-S (Imaging) mode), as discussed in Weisskopf et al..[1]

3.1. Structure

Figure 4 shows the observation of 3C58 taken with the HRC-S(Imaging) as discussed by Murray et al..[9] The panel on the left is an adaptively smoothed image at a scale of 1 arc second per pixel and shows the large scale features of this object which extends about ±2 arc minutes. The extended shell contains a bright, but extended, central region shown on an expanded scale (0.13 arc seconds per pixel) in the right side of the figure. Embedded in this extended inner feature is a point source which is the putative pulsar. The inner region was fit to a multicomponent spatial model, including a point source, a two dimensional extended source (with Gaussian distributions in both axes) and a constant background. Alternatively a model for this inner region similar to that observed for the Crab Nebula (Weisskopf et al.[10]) could consist of a point source and a torus corresponding to the pulsar wind nebula termination shock, and a constant background as discussed by Slane, Helfand and Murray.[11] Depending on the true spatial distribution, we may be observing the point source directly, or through an extended nebula.
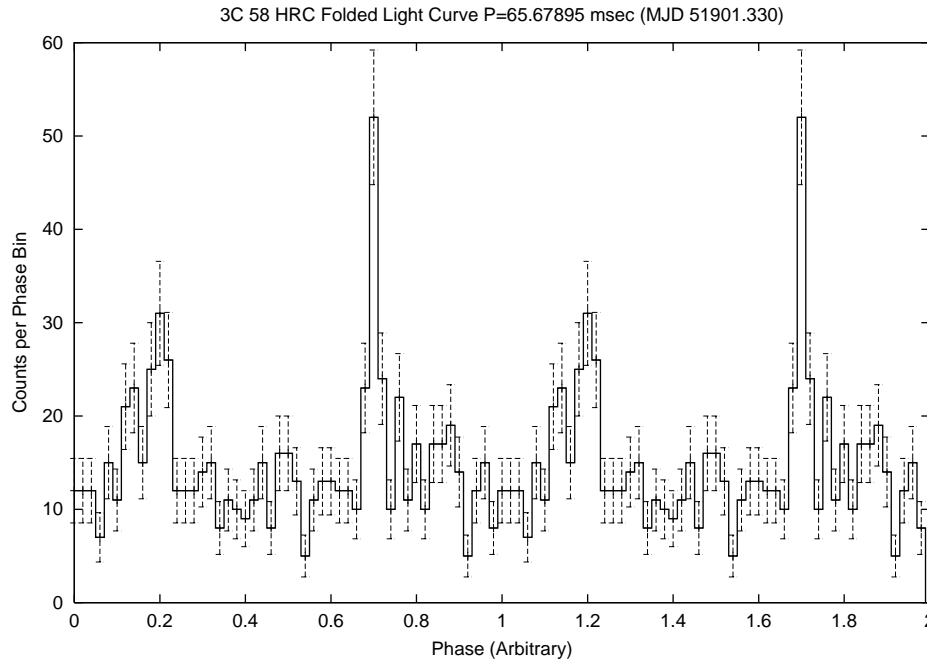
Figure 5. HRC-S pulse profile. The period is about 65 msec, and each phase bin is about 1.3 msec.

3.2. Timing

Events from the point source were selected by setting a 1 arc second radius region at the position of the source. A total of 744 events were obtained from the 33 ksec observation for timing analysis. Time corrections are applied to convert the photon arrival times to the Barycentric Dynamical Time (TDB) reference system and then an FFT was run on the time ordered event list to search for possible periods followed by more detailed analysis of the candidate periods as described by Murray et al..[9] A pulse period of about 65 msec was found with high confidence and the resulting pulse profile (or light curve) is shown in Figure 5. The profile consists of two sharp pulses, the main pulse has a width of about 2 msec while the broader inner pulse has a width of about 3-4 msec. With the discovery of pulsations the point source is now designated PSR J0205+6449. Once the Chandra data detected this pulse period the pulsar was also detected at radio wavelengths using the 100 m dish at Green Bank (Camilo et al.[12]). The pulsations were also recovered from archival RXTE data as discussed by Murray et al.,[9] which allowed not only the period but the spin down rate to be measured. Since this is a pulsar whose age is known (the supernova was recorded in 1181 AD and was therefore, 820 years old when the period was measured), the observed period and spin down rate allow the pulsar magnetic field to be estimated ($B \sim 3.6 \times 10^{12}$G), and the initial spin period (~60 msec) to be calculated. While 3C58 is similar in many ways to the archetype pulsar in a young supernova remnant, the detailed characteristics obtained from the Chandra data indicate striking and important differences that remain unexplained and will require both more observational data, and better theoretical models.

3.3. Neutron Star Cooling

Using a combination of Chandra HRC timing results discussed above and a 34 ksec ACIS-S detector to study the spectral properties of the 3C58 SNR and pulsar, we have been able to estimate a conservative upper limit to the surface temperature of the neutron star and compare it with theoretical calculations.

Using the pulse profile obtained with the HRC, we can place an lower limit to the fraction of flux that is pulsed and therefore coming from a region above the surface of the neutron star. Most likely these X-rays are emitted in the neutron star magnetosphere and have a power law spectrum similar to the extended nebula
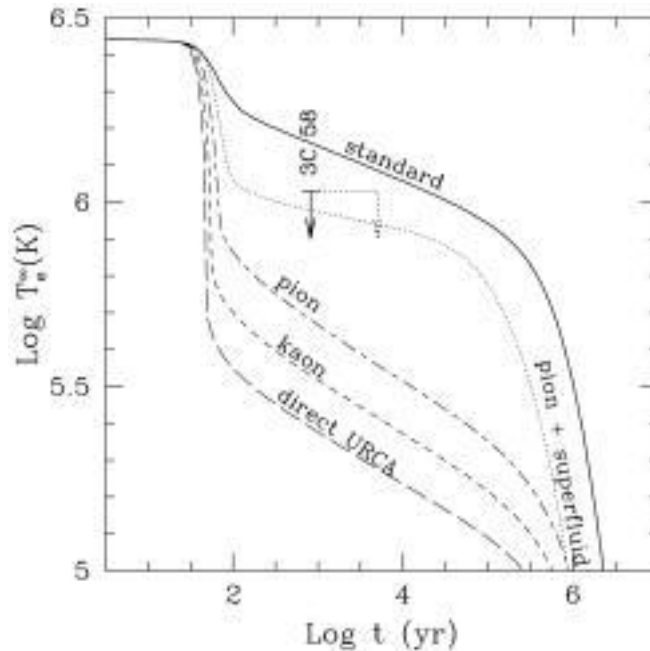
Figure 6. Cooling curves for neutron stars with the upper limit surface temperature for J0205+6449. Taken from Slane, Helfand, and Murray[10]. NS Model data are taken from Page[12].

($\Gamma = 1.73 \pm 0.07$). Converting this flux into equivalent ACIS counts allows us to subtract from the total ACIS point source intensity that part which is not emitted from the surface of the neutron star. This difference gives an upper limit to the surface emission, $f_x = 1.54 \times 10^{-2}$c s^{-1}. For a blackbody with radius (at infinity) of 12 km, and an absorption column of $N_H = 3.75 \pm 0.11 \times 10^{21}$cm^{-2}, the upper limit to the blackbody temperature corresponding to this flux is 1.13×10^6K. This is a conservative upper limit because we have only considered the minimum pulsed data, and because the blackbody spectral shape over estimates the actual surface temperature for emission from the neutron star surface.

This temperature can be compared to theoretical calculations (summarized by Page[13]) for the temperature of an 820 year old neutron star under various assumptions. This is shown in Figure 6. As discussed by the authors, it is clear that the neutron star in 3C58 is too cool to be described by the so called "standard" cooling models, and that some more exotic model is needed. Possible explanations for the low temperature of this neutron star range from the presence of exotic processes in the core that enhance neutrino emission, to the neutron star being slightly more massive than expected (Yakovlev et al.[14]). Further observations with Chandra to improve on the measurements already made are being planned to help investigate these alternatives.

4. COMPLEX X-RAY EMISSION FROM CENTAURUS A

The nearest Active Galactic Nucleus source is Centaurus A (Cen A) $\sim$3.4 Mpc from Earth. This is a well studied object with observations at virtually all wavelengths (Israel[15]). Previous to the Chandra studies, it was already known that the super massive black hole ($2 - 3 \times 10^8 M_\odot$) powers an FR-I radio source and a jet that extends $\sim$6 kpc (6 arc minutes) from the nucleus. X-ray studies of Cen A using the *Einstein, ROSAT,* and *ASCA* observatories (c.f. Turner et al.[16] and references therein) have detected X-ray emission along most of the radio jet with bright enhancements coincident with the radio knots of the inner jet. With the excellent spatial and spectral resolution of Chandra (and with supporting observations using XMM and HST) we have been able to study the properties of the jet in great detail (Kraft et al.[17]). Figure 7 shows the Chandra image of Cen A obtained using the ACIS-I as part of the HRC GTO program. This image combines two 36 ksec observations (OBSID00316 and OBSID00962) taken 5 months apart (December 5, 1999 and May 17, 2000).
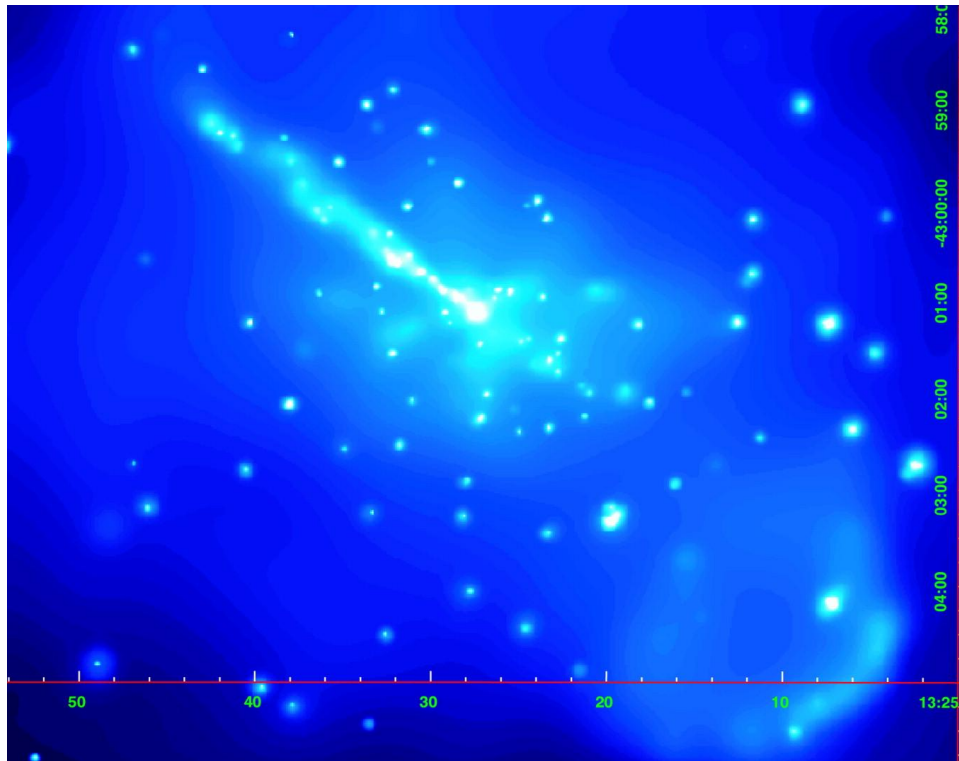
Figure 7. Adaptively smoothed, co-added, exposure corrected Chandra X-ray image of Cen A in the 1-3 keV energy band. The nucleus is the bright source near the center of the field, the jet extends to the northeast and is about 4 kpc long.

Many of the features of Cen A are apparent in Figure 7. The bright central source is associated with the nucleus and the super massive black hole. The jet extends about 4 kpc toward the northeast and is made up of individual knots of bright emission embedded in a continuum of radiation. There are many point sources associated with the galaxy as well as diffuse emission from the hot ISM around the nucleus. Finally there is an extended emission feature to the southwest that is coincident with one of the inner radio lobes. All of these features are being studied in detail (c.f. Kraft et al.[17, 18]).

4.1. Jet

A detailed view of the inner jet of Cen A is seen in Figure 8. The X-ray emission is mainly in the form of bright knots, such as AX1 and BX2, which are unresolved by Chandra and many additional fainter features and knots some of which are resolved. There is also a diffuse component along the jet which can be seen after subtraction of the more localized features or via a wavelet decomposition. At the resolution of Chandra it can be seen that while the radio knot A1 (Burns et al.[19]) corresponds well with AX1, there is poorer correspondence for the other radio knots, and that the X-ray features tend to lie closer to the nucleus than their corresponding radio features. These observations suggest that the X-ray emission in this jet is not simply synchrotron radiation but, as discussed in Kraft et al.,[17] there is particle acceleration along the jet with the knots being shocked regions.

4.2. Radio Lobe

On a larger scale, the X-ray emission associated with the southwest radio lobe is seen more clearly in Figure 9. Here the adaptively smoothed X-ray image (0.5-2 keV) around the southwest radio lobe is shown with the 13 cm radio contours overlaid. Kraft et al.[18] suggest that the X-ray emission is from a shell of thermal plasma that surrounds the radio lobe and that the enhancement is due to edge brightening effects. This shell
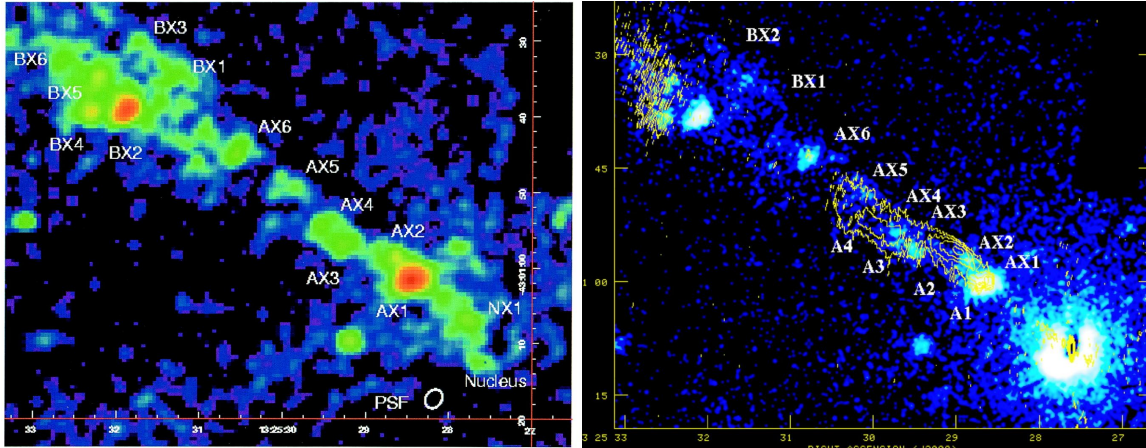
Figure 8. The inner jet of Cen A. The left side is the Chandra X-ray image in the 0.4-1.5 keV band to emphasize the jet emission relative to the nucleus. The image contains data from OBSID00316 and has been smoothed by a Gaussian with a 0.5 arc second sigma. The knots are labeled for comparison with the radio designations. On the right side is the 0.5-5 keV image, also smoothed with a 0.5 arc second sigma Gaussian. Radio contours from the VLA 3.6 cm observation are plotted over X-ray image.
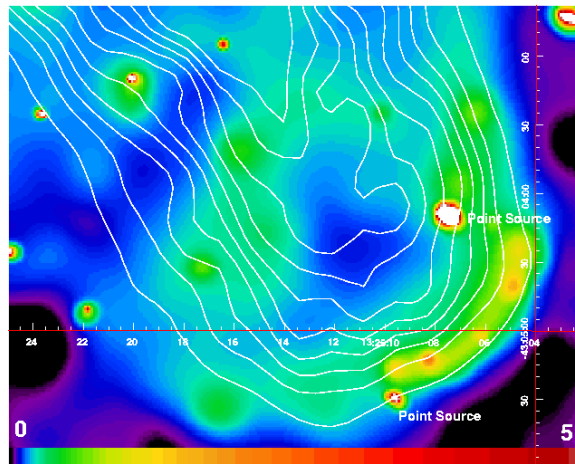
Figure 9. Detailed view of the X-ray emission (0.5 -2 keV) from the Southwest radio lobe and the 13 cm VLA image contours. The colors indicate X-ray surface brightness in units of $10^{-5}\,\mathrm{cts\,arcsec^{-2}\,s^{-1}}$. The radio contours correspond to a flux density of 0.03 - 2 Jy/beam in ten logarithmic steps.

of plasma is the result of the expansion of the radio lobe into the ISM, which displaces and compresses the ISM as the lobe expands. The shell is thin and over pressurized indicating that the radio lobe is expanding supersonically. Otherwise the shell would have time to dissipate, particularly sharp features such as those at the edge. More detailed work remains to be done to fully understand the conditions associated with this model and the possibility that similar processes are being observed in radio plasma/ICM interactions in early galaxies as seen by Chandra and XMM (e.g., Finoguenov and Jones,[20] Jones et al.[21]).

4.3. Arcs

An early Chandra HRC-I image of Cen A was taken in September 1999 (OBSID00463) as part of the Orbital Activation and Calibration phase of the mission. Figure 10 taken from Karovska et al.[22] is a 16 x 16 arc minute
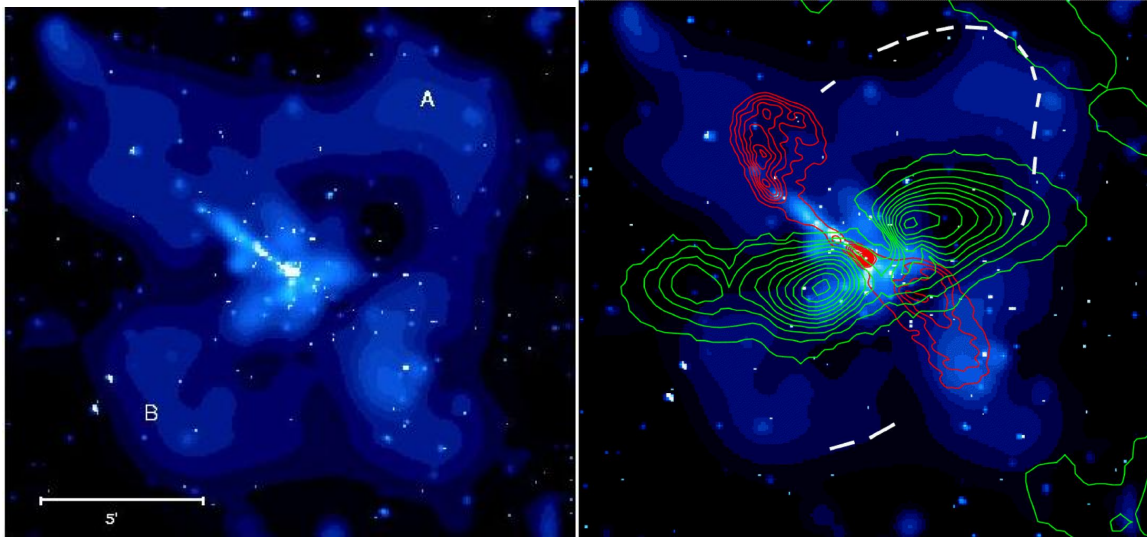
Figure 10. Adaptively smoothed HRC-I image of Cen A. On the left only the X-ray image is shown. On the right, the red contours are from the VLA 21 cm continuum showing the jet and radio lobes, the green contours are from VLA 21 cm HI line emission from cool material. The white dashed line is a schematic representation of the optical arc-like shell seen in the enhanced blue DSS image.

field of view taken from the adaptively smoothed image using the *csmooth* tool from the CXC CIAO data analysis package[†]. The X-ray image reveals several spatial components, and in particular we point out the large scale diffuse emission that extends out to ~10 arc minutes approximately perpendicular to the jet. The most striking features of the of this large scale x-ray emission are the two arc-like structures A in the northwest and B in the southeast as shown in Figure 10. They appear symmetric about an axis perpendicular to the direction of the jet. As discussed by Karovska et al.,[22] the X-ray arcs trace an ellipse which can be interpreted as ring or torus -like structure seen in projection (inclined at $60 - 70°$ from the plane of the sky). The X-ray spectrum of these arcs was obtained from the ACIS-I observations discussed above, and yield a low temperature ($kT \sim 0.4 - 0.6$ keV, depending on the value of N_H). One interpretation of this observation is that the X-ray ring is a result of an interaction between an equatorial outflow or wind from the nucleus of Cen A and the galactic ISM, perhaps triggered from some transient nuclear activity. In this scenario, Karovska et al. estimate that the outburst occurred $\sim 10^7$ years ago and lasted for $\sim 3 \times 10^4$ years. These ages are consistent with the young age of stars in the optical arc (Peng et al.[23]) and the estimated age of the current burst of star formation in Cen A (Israel[15]).

5. CONCLUSIONS AND ACKNOWLEDGMENTS

The first three years of observations with Chandra have provided a wealth of new information for the HRC Team to digest. Using the GTO allocation of time we have sampled numerous astrophysical phenomena ranging from the formation of stars to the evolution of clusters of galaxies. The examples given in this presentation barely scratch the surface of the discoveries that have been made with Chandra these past few years. We look forward to continuing an exploration of cosmic X-ray sources and the new insights which will come. The HRC Team is grateful for the support we receive from NASA (NAS8-38248 and NAS8-01130) and to the Chandra Operations Control Center (OCC) and the Chanda X-ray Center (CXC) for all of the support provided to carry out our observations and process the data.

[†]CIAO is the Chandra Interactive Analysis of Observations data analysis systems package available at http://cxc.harvard.edu/ciao. *Csmooth* is adapted from the *asmooth* routine developed by Harald Ebeling.

REFERENCES

1. M. Weisskopf *et al.*, "An overview of the performance and scientific results from the Chandra X-ray Observatory," *PASP* **114**, pp. 1–24, 2002.

2. P. Freeman *et al.*, "A wavelet based algorithm for the spatial analysis of Poisson data," *ApJS* **138**, pp. 138–158.

3. A. Kong *et al.*, "Two years of the x-ray sky in M31," in *Proceedings of the Symposium New Visions of the X-ray Universe in the XMM-Newton and Chandra Era*, pp. 26–30, November.

4. A. Kong *et al.*, "X-rya point sources in the central region of M31 as seen by Chandra." submitted to ApJ, 2002.

5. F. Primini, W. Forman, and C. Jones, "High-resolution x-ray observations of the central region of M31 with the ROSAT satellite," *ApJ* **410**, pp. 615–625, 1993.

6. A. Dosaj *et al.*, "Diffuse emission in the nucleus of M31," *BAAS* **199**(46.02), 2001.

7. M. Garcia *et al.*, "A first look at the nuclear region of M31 with Chandra," *ApJ* **537**, pp. L23–26, 2000.

8. M. Garcia *et al.*, "Chandra observations of M31* and M31 transients," in *Two Years of Science with Chandra*, September 2001.

9. S.S.Murray *et al.*, "Discovery of x-ray pulsations from the compact central source in the supernova remnant 3c58," *ApJ* **568**, pp. 226–231, 2002.

10. M.C.Weisskopf *et al.*, "Discovery of spatial and spectral structure in the x-ray emission from the Crab Nebula," *ApJ* **536**, pp. L81–L84, 2000.

11. P. Slane, D. Helfand, and S. Murray, "New constraints on neutron star cooling from Chandra observations of 3C58," *ApJ* **571**, pp. L45–L49, 2002.

12. F. Camilo, "Discovery of radio pulsations from the x-ray pulsar J0205+6449 in supernova remnant 3C58 with the green bank telescope," *ApJ* **571**, pp. L41–L44, 2002.

13. D. Page, *The Many Faces of Neutron Stars*, pp. 539–. Dordrecht: Kluwer, 1998.

14. D. Yakovlev, A. Kaminker, P. Haensel, and O. Gnedin, "The cooling neutron star in 3C58," *A&A* **389**, pp. L24–L27, 2002.

15. F. Isreal, "Centaurus A - NGC 5128," *A&A* **Rev 8**, pp. 237–278, 1998.

16. T. Turner *et al.*, "Deconvolution of the x-ray emission and absorption components in Centaurus A," *ApJ* **475**, pp. 118–133, 1997.

17. R. Kraft *et al.*, "Chandra observations of the x-ray jet in Centaurus A," *ApJ* **569**, pp. 54–71, 2002.

18. R. Kraft *et al.*, "X-ray emission from the hot ISM and inner radio lobes of the nearby radio galaxy Centaurus A." in preperation, 2002.

19. J. Burns, E. Fiegelson, and E. Schreier, "The inner radio structure of Centaurus A - clues to the origin of the jet x-ray emission," 1983.

20. A. Finoguenov and C. Jones, "Chandra observation of M84, a radio lobe elliptical galaxy in the Virgo Cluster," *ApJ* **547**, pp. L107–110, 2001.

21. C. Jones *et al.*, "Chandra observations of NGC 4636-an elliptical galaxy in turmoil," *ApJ* **567**, pp. L115–118, 2002.

22. M.Karovska *et al.*, "X-ray arc structures in Chandra images of NGC5128 (Centaurus A)." accepted for publication in ApJ, 2002.

23. E. Peng, H. Ford, and K. Freeman, "A young tidal stream in NGC 5128 (Cen A)," *BAAS* **199**.